

Design of Tri-Band Hybrid Dielectric Resonator Antenna for Wireless Applications

Lavuri Nageswara Rao^{1, 2, *},
Govardhani Immadi¹, and Madhavareddy Venkata Narayana¹

Abstract—In this article, a compact dielectric resonator antenna (DRA) with partial ground plane for wireless applications is examined. The exhibited structure is fed by a microstrip line. To demonstrate the functionality of a tri-band, a circular dielectric resonator antenna with concentric circular rings is created. The developed antenna parametric analysis has been performed on HFSS platform. The configured design operates at three frequency bands, i.e., 1.98–2.59 GHz (ISM), 3.24–3.85 GHz (Wi-max), and 4.85–5.85 GHz (WLAN), with the fractional bandwidths of 26.6%, 20.4%, and 18.67%, respectively. The customized concentric rings are placed onto the substrate to reinforce the antenna appearance and also miniaturize the size. The measured outcomes are strongly in accordance with the simulated results. The designed model can be customized with certain attributes to wireless applications.

1. INTRODUCTION

Dielectric Resonator Antennas (DRAs) [1] have been described for advanced wireless technologies as potentially useful antennas. Particularly in contrast with microstrip antennas, it provides features such as improved efficiency, high bandwidth, low volume, low production costs, and ease of fabrication. DRA is an absolutely enticing solution of wireless technology. In recent years, many researchers have described theoretical and experimental studies on DRAs with cylindrical, rectangular, and hemispherical types [2–8].

DRAs are adopted by utilizing feeding methods, like coplanar waveguide, probe, and microstrip line [9]. In this approach, a microstrip feed line is directly connected to a resonator to provide planar structure [10], and it provides more flexibility. The concentric rings of the implemented feeding structure are placed onto the substrate to improve the antenna characteristics. The adapted feed line dielectric resonator antenna with partial ground plane in the ISM band, WiMAX, and WLAN for wireless applications is implemented. A composite dielectric resonator [11–15] is involved in the described configuration. Concentric circular rings are desired for the creation of multi-band properties owing to their basic configuration. This is additionally utilized for tuning the range of frequency for antenna [16–18]. By stacking the composite materials, size of the antenna is reduced. In recent years, there has been a tremendous improvement in wireless applications, particularly in ISM, WiMAX, and WLAN bands. To resolve therapeutic conflicts in wireless body area networks (WBAN) [19–25], WiMAX/WLAN is utilized. The studied outcomes of the developed structure explicitly encourage the WBAN applications in wireless technology.

In this work, a miniature composite dielectric resonator is aimed to acquire tri-band [27, 28] functionality in wireless applications. The primary target of this paper is to accomplish tri-band attributes [29, 30] with the assistance of the implemented antenna, i.e, circular DRA and concentric

Received 25 March 2021, Accepted 3 June 2021, Scheduled 18 June 2021

* Corresponding author: Lavuri Nageswara Rao (lavurinagesh@gmail.com).

¹ Department of Electronics and Communication Engineering, KoneruLakshmaiah Education Foundation, Guntur, Andhra Pradesh 522502, India. ² CVR College of Engineering, Hyderabad, India.

circular rings. The configured structure is suitable for ISM, WiMAX, and WLAN. An intended structure is compact and simple, and it is also customized to wireless applications. The analysis of an implemented antenna is performed on HFSS platform.

2. ANTENNA CONFIGURATION

Figure 1 depicts the structure of dielectric resonator geometry. It explores the adapted feed line dielectric resonator antenna with partial ground plane in the ISM band, WiMAX, and WLAN for wireless applications. The exhibited configuration is sustained by a microstrip feed line.

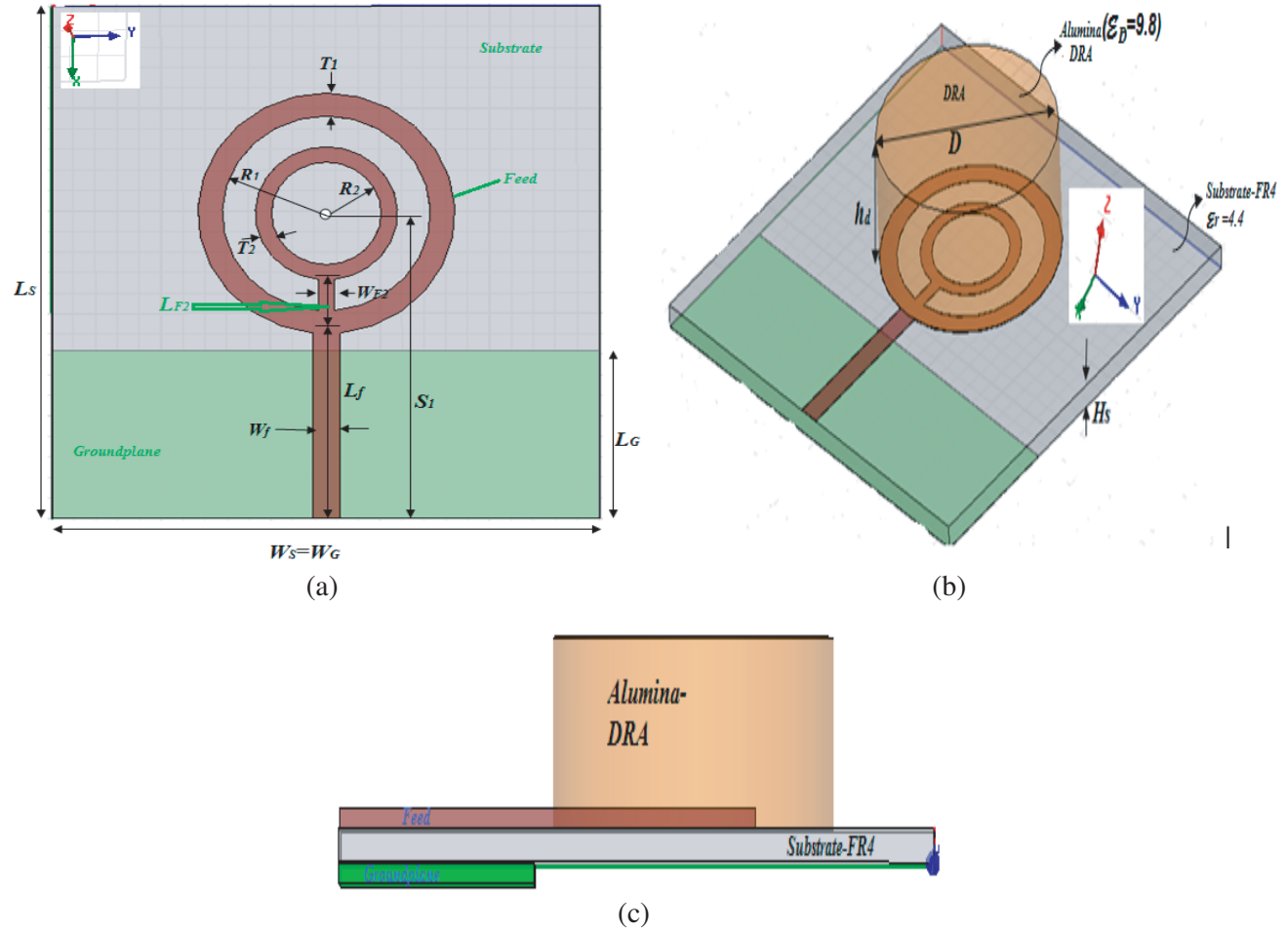


Figure 1. Configuration of designed DRA: (a) Feeding structure; (b) 3-D view; (c) side view.

The developed concentric rings are placed onto the substrate to improve the antenna characteristics and to reduce the size of the antenna. The external ring generates the ISM band; DRA is responsible for the creation the WiMAX, and WLAN band is delivered because of the common endeavors of DRA and internal ring structure. The fabricated model of proposed DRA is exhibited in Fig. 2.

The geometry of substrate-FR4 is 50 mm*50 mm. The relative permittivity of substrate is $\epsilon_r = 4.4$, and its thickness is $h = 1.6$ mm. The DRA is tightly stacked with a substrate based concentric circle patch to generate the WiMAX (3.5 GHz) and WLAN (2.38 GHz & 5.4 GHz) frequency ranges. From Fig. 1, it is observed that the first band is due to the outer ring, second band due to the CDRA, and the cross shaped element is responsible for the third band. Table 1 demonstrates the geometry of proposed structure.

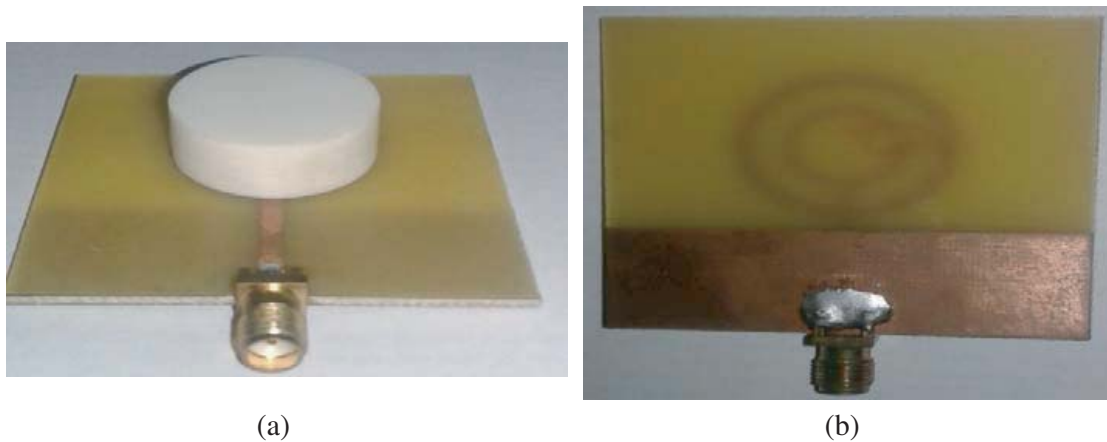


Figure 2. Prototype of CDRA: (a) Isometric view; (b) Bottom view.

Table 1. Dimensions of proposed antenna.

Basic configuration	Parameters	Value (mm)	Materials used
Ground plane	L_G	16.4	Copper
	W_G	50	
Substrate	L_S	50	FR-4 ($\epsilon_r = 4.4$)
	W_S	50	
	H_S	1.6	
Feed: Outer ring	L_f	18.5	Copper
	W_f	2.5	
	L_{f2}	5.5	
	W_{f2}	1.5	
	R_1	9	
	T_1	2.25	
Inner ring	R_2	5	Copper
	T_2	1.5	
	S_1	29.75	
Circular DRA	D	23.5	Alumina ($\epsilon_d = 9.8$)
	h_d	9	

According to [12], the resonant frequency of a DRA is assessed as follows, and it is equivalent to 3.5 GHz.

$$f_r = \frac{c}{2\pi R} \left(\frac{1.6 + 0.513x + 1.392x^2 - 0.577x^3 + 0.088x^4}{\epsilon_d^{0.42}} \right) \tag{1}$$

$$x = \frac{R}{2h_d} \tag{2}$$

where c is the speed of light; h_d , ϵ_d and R are height, relative permittivity, and radius of the DRA, sequentially.

The theoretical resonant frequencies for outer and inner rings are analyzed as follows [26], and the following equations are considered for both the resonant frequencies, i.e., outer ring and inner ring

generate the frequencies of 2.4 GHz and 5.2 GHz, respectively.

$$f_{ring} = \frac{Ac}{2\pi R\sqrt{\epsilon_{re}}} \quad (3)$$

$$A = \frac{2R}{(R+T)+R} \quad (4)$$

$$\epsilon_{re} = \frac{1}{2}(\epsilon_{r,sub} + 1) + \frac{1}{2}(\epsilon_{r,sub} - 1)\left(1 + \frac{10H_S}{T}\right)^{-\frac{1}{2}} \quad (5)$$

where ϵ_{re} and ϵ_r are effective relative permittivity and substrate permittivity sequentially. H_S is the substrate height, R the circular ring radius, and T the thickness.

3. PARAMETRIC ANALYSIS

Simulation studies of the proposed antenna have been carried out by using Ansys HFSS simulator. This section focuses on exploring and understanding of development of three frequency ranges.

3.1. Impact of Ground Plane Length

The variation of return loss characteristics with various ground plane lengths is exhibited in Fig. 3. It tends to be seen from Fig. 3 that the resonance of different frequencies becomes destitute when ground plane length is increased, and it also brings the desired radiator absolutely analogous to non-resonance. To acquire better resonance, length of ground plane is chosen as 16.4 mm.

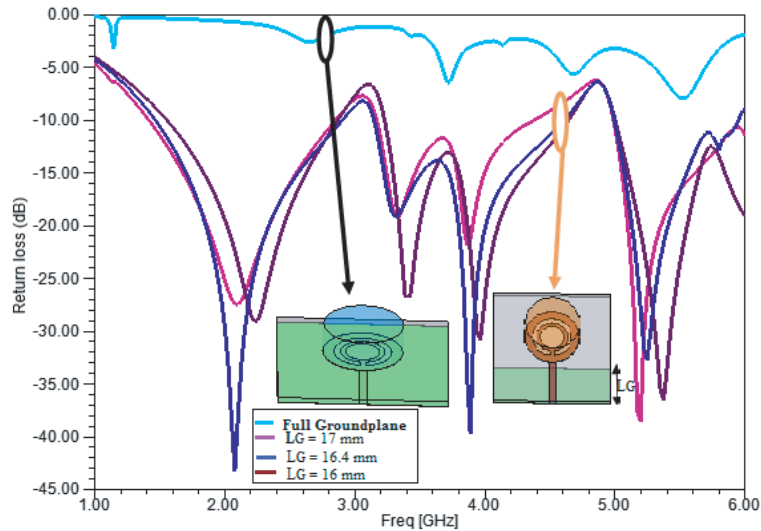


Figure 3. Simulated return loss with various ground plane length.

3.2. Different Radiating Structure

Return loss characteristics with different radiating models are illustrated in Fig. 4. From Fig. 4, it can be observed that outer circular ring generates the 2.38 GHz frequency band. Moreover, the 5.4 GHz frequency is generated due to the inner circular ring, and DRA is responsible for the generation of 3.5 GHz frequency. These resonances were also observed in Section 2 theoretically.

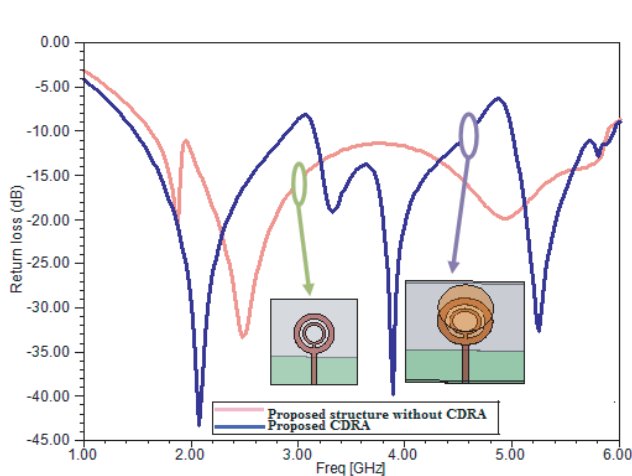


Figure 4. Simulated return loss without and with DRA.

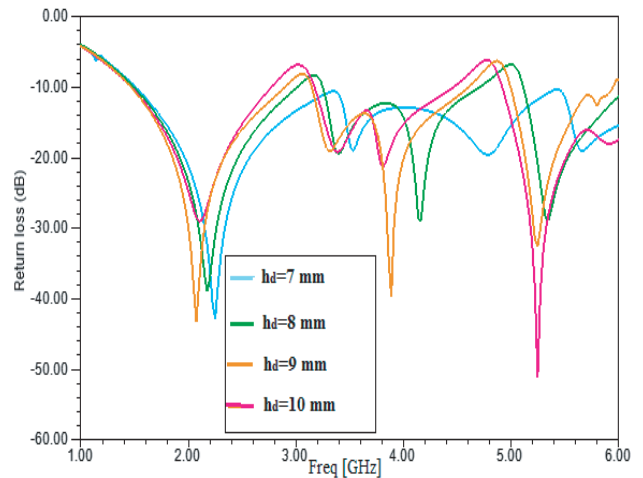


Figure 5. Return loss characteristics for various heights of DRA.

3.3. DRA Height

Return losses with different DRA heights are exhibited in Fig. 5. From Fig. 5, it can be seen that as the height increases the resonant frequency decreases. From this observation, it is implied that the height of the DRA significantly affects the mid-frequency.

4. MEASURED RESULTS AND DISCUSSION

To validate the model, a prototype of intended antenna is fabricated and measured as illustrated in Fig. 2. The vector network analyzer has been utilized to acquire the attributes of the developed structure. The return loss is another method of communicating mismatch. It is a logarithmic proportion estimated in dB that analyzes the power reflected by the receiving wire to the power that is bolstered into the radio wire from the transmission line.

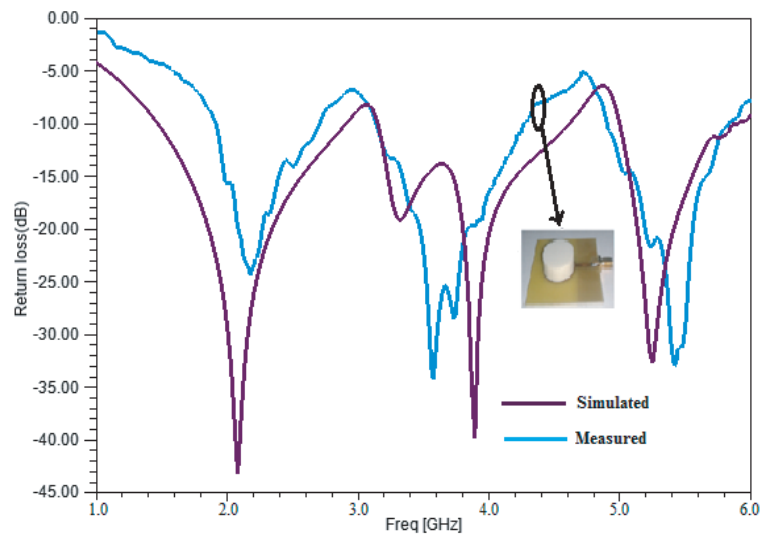


Figure 6. Simulated and measured return loss of proposed antenna.

Simulated and measured return losses of the suggested antenna are exhibited in Fig. 6. As illustrated in Fig. 6, the prototype design operates at three different frequency bands, i.e., 1.98–2.59 GHz, 3.24–3.85 GHz, and 4.85–5.85 GHz, with fractional bandwidths of 26.6%, 20.4%, and 18.67%, respectively. The measured outcomes are strongly in accordance with the simulated results.

Table 2 illustrates the comparison of the designed DRA with various established DRA models based on impedance bandwidth, and it depicts that the implemented DRA has a wide impedance bandwidth compared to the established antenna structures [31–34].

The radiation pattern of antenna gives the data that depict how the reception apparatus coordinates the vitality it transmits. All antennas, if 100% efficient, radiate the same total energy for equal input power regardless of pattern shape. Simulated gain of the intended structure is illustrated in Fig. 7. The developed DRA gains at 2.4 GHz, 3.5 GHz, and 5.4 GHz are about 2.4 dBi, 4.13 dBi, and 3.5 dBi, respectively. From Fig. 7, it can be seen that the gain at 3.5 GHz is better than that at 5.2 GHz. The developed model has good radiation characteristics at three frequencies.

The proposed antenna is simulated by using HFSS tool. Fig. 8 demonstrates the simulation model on HFSS platform, which consists of the designed DRA and simulated results. The simulated model generates three frequency bands, and it can be observed in Fig. 8.

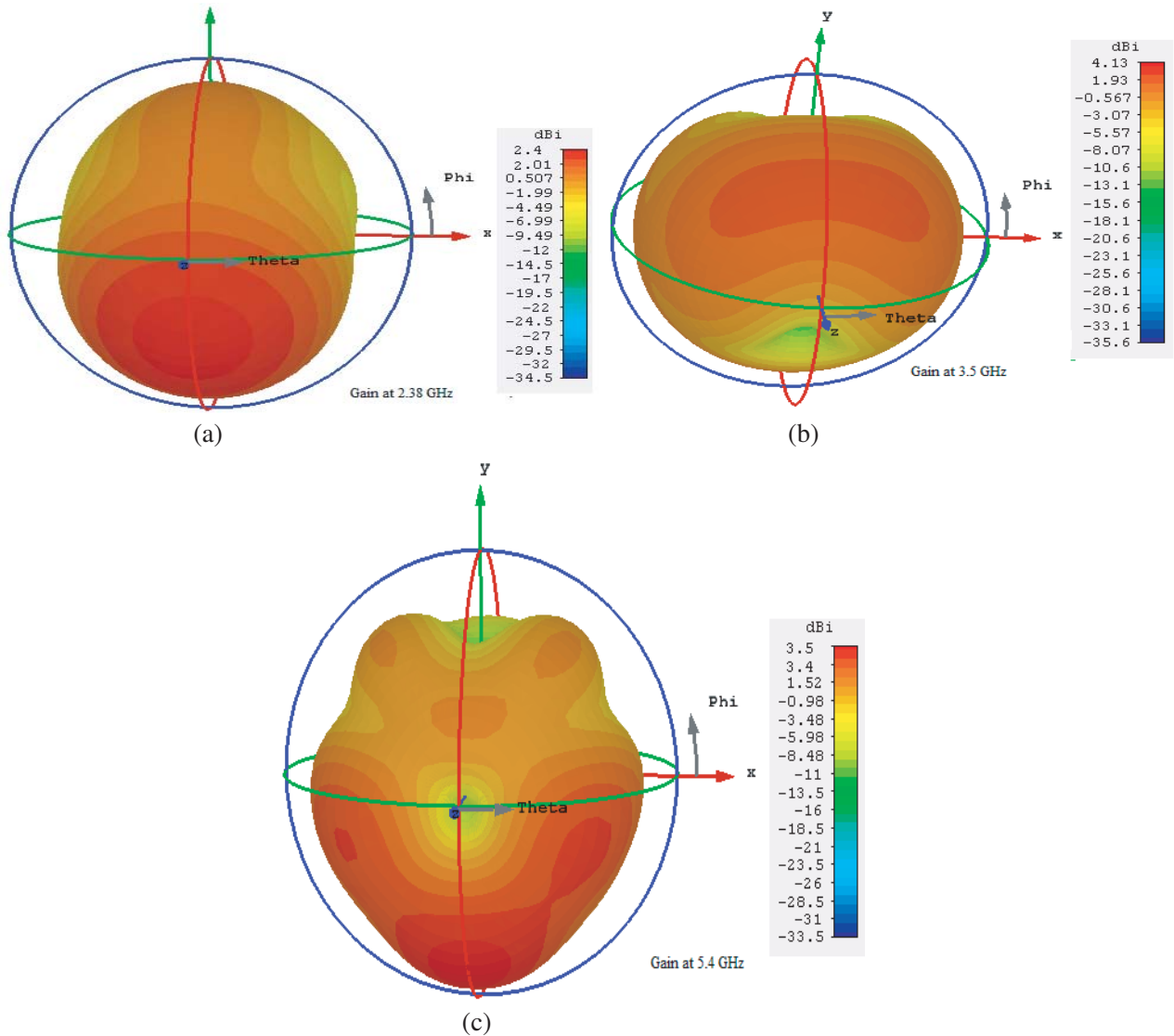


Figure 7. Simulated gain at: (a) 2.38 GHz; (b) 3.5 GHz; (c) 5.4 GHz.

Table 2. Comparison of proposed structure with various existing DRA structures.

DRA shape	Feed type	Lower band		Middle band		Upper band	
		frequency (GHz)	bandwidth (%)	frequency (GHz)	bandwidth (%)	frequency (GHz)	bandwidth (%)
Modified RDRA [31]	Microstrip line	2.4	3.39	3.5	11.1	5.8	1.7
CDRA [32]	CPW	2.4	16.5	3.5	4.5	5.2	20.9
RDRA [33]	Co-axial feed	-	-	3.5	9.97	5.25	8.8
RDRA [34]	Microstrip line	2.45	25	-	-	5.2	13
Proposed Antenna	Microstrip line	2.4	26.6	3.5	20.4	5.4	18.67

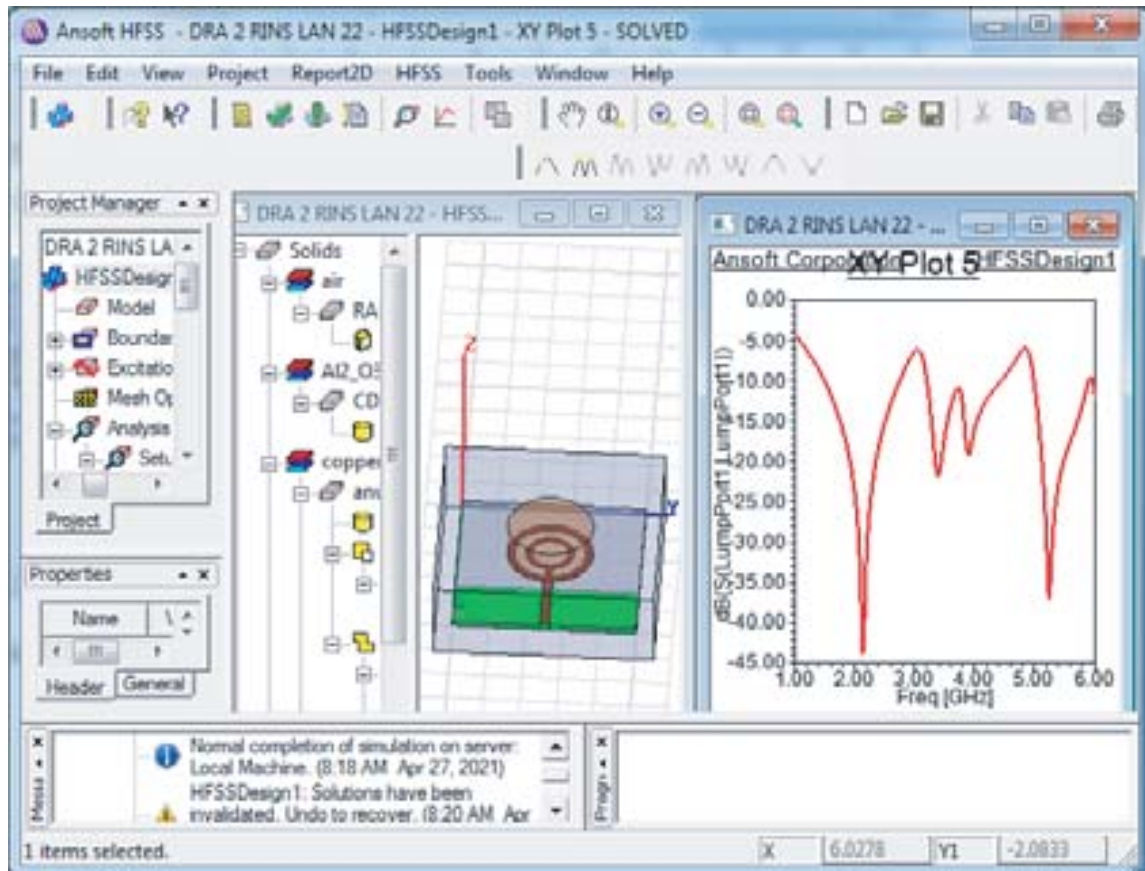


Figure 8. Simulated results on HFSS platform.

5. CONCLUSION

A miniature tri-band composite dielectric resonator antenna is examined for wireless applications. Creating tri-band frequencies, i.e., ISM (1.98–2.59 GHz), WiMAX (3.24–3.85 GHz), and WLAN (4.85–5.85 GHz), is a key feature of the implemented framework. The system was implemented and fabricated and discovered to have fractional bandwidths of 26.6%, 20.4%, and 18.67% at 2.38 GHz, 3.5 GHzs and 5.4 GHz resonant frequencies, respectively. The implemented antenna demonstrates great radiation characteristics for the deployed structure's three functional bands. The obtained configuration is very compact and easy. The proposed approach can be adapted to wireless applications with these characteristics. Future research will focus on stacked dielectric resonators antenna. The dielectric resonators can be combined to improve the impedance bandwidth of the stacked DRA model, and it can be support the multiband behavior.

REFERENCES

1. Kishk, A. A., B. Ahn, and D. Kajfez, "Broadband stacked dielectric resonator antennas," *Electron. Lett.*, Vol. 25, 1232–1233, Aug. 1989.
2. Varshney, G., S. Gotra, V. S. Pandey, and R. S. Yaduvanshi, "Inverted-sigmoid shaped multiband dielectric resonator antenna with dual-band circular polarization," *IEEE Transactions on Antennas and Propagation*, Vol. 66, No. 4, 206–2082, Apr. 2018.
3. O'Connor, E. M. and S. A. Long, "The history of the development of the dielectric resonator antenna," *ICEAA International Conference on Electromagnetics in Advanced Applications*, 872–875, Turin, Italy, Sept. 2007.
4. Simons, R. N. and R. Q. Lee, "Effect of parasitic dielectric resonator on CPW/aperture-coupled dielectric resonator antenna," *Proc. Inst. Elect. Eng., Microw. Antennas Propag.*, Vol. 140, 336–338, Oct. 1993.
5. Chen, H.-M., Y.-K. Wang, Y.-F. Lin, S.-C. Lin, and S.-C. Pan, "A compact dual-band dielectric resonator antenna using a parasitic slot," *IEEE Antennas and Wireless Propagation Lett.*, Vol. 8, 173–176, Apr. 2009.
6. Song, Z., H. Zheng, M. Wang, Y. Li, T. Song, E. Li, and Y. Li, "Equilateral triangular dielectric resonator and metal patch hybrid antenna for UWB application," *IEEE Access*, Vol. 7, 119060–119068, 2019.
7. Afifi, A. I., A. B. Abdel-Rahman, A. S. A. El-Hameed, A. Allam, and S. M. Ahmed, "Small frequency ratio multi-band dielectric resonator antenna utilizing vertical metallic strip pairs feeding structure," *IEEE Access*, Vol. 8, 112840–112845, 2020.
8. Fatah, S. Y. A., E. K. I. K. I. Hamad, W. Swelam, A. M. M. A. Allam, M. F. Abo Sree, and H. A. Mohamed, "Design and implementation of UWB slot-loaded printed antenna for microwave and millimeter wave applications," *IEEE Access*, Vol. 9, 29555–29564, 2021.
9. Leung, K. W., K. Y. Chow, K. M. Luk, and E. K. N. Yung, "Low-profile circular disk DR antenna of very high permittivity excited by a Microstrip line," *Electron. Lett.*, Vol. 33, 1004–1005, Jun. 1997.
10. Kranenburg, R. A. and S. A. Long, "Microstrip transmission line excitation of dielectric resonator antennas," *Electron. Lett.*, Vol. 24, 1156–1157, Sept. 1988.
11. So, K. K. and K. W. Leung, "Bandwidth enhancement and frequency tuning of the dielectric resonator antenna using a parasitic slot in the ground plane," *IEEE Transactions on Antennas and Propagation*, Vol. 53, No. 12, 4169–4172, Dec. 2005.
12. Huitema, L., M. Koubeissi, C. Decroze, and T. Monediere, "Compact and multiband dielectric resonator antenna with reconfigurable radiation pattern," *Proc. 4th Eur. Conf. Antennas Propag.*, 1–4, Apr. 2010.
13. Leung, K. W. and K. K. So, "Frequency-tunable designs of the linearly and circularly polarized dielectric resonator antenna using a parasitic slot," *IEEE Transactions on Antennas and Propagation*, Vol. 53, No. 1, 572–576, Jan. 2005.

14. Wu, Q., "Characteristic mode assisted design of dielectric resonator antennas with feedings," *IEEE Transactions on Antennas and Propagation*, Vol. 67, No. 8, 5294–5304, Aug. 2019.
15. Lin, I. K. C., M. H. Jamaluddin, A. Awang, R. Selvaraju, M. H. Dahri, L. C. Yen, et al., "A triple band hybrid MIMO rectangular dielectric resonator antenna for LTE applications," *IEEE Access*, Vol. 7, 122900–122913, Aug. 2019.
16. Denidni, T. A. and Q. Rao, "Hybrid dielectric resonator antenna with radiating slot for dual-frequency operation," *IEEE Antennas and Wireless Propagation Lett.*, Vol. 3, 321–323, Dec. 2004.
17. Elek, F., R. Abhari, and G. V. Eleftheriades, "A uni-directional ring-slot antenna achieved by using an electromagnetic band-gap surface," *IEEE Transactions on Antennas and Propagation*, Vol. 53, 181–190, Jan. 2005.
18. Row, J. S. and S. W. Wu, "Circularly-polarized wide slot antenna loaded with a parasitic patch," *IEEE Transactions on Antennas and Propagation*, Vol. 56, 2826–2832, Sept. 2008.
19. Salonen, P. and L. Hurme, "A novel fabric WLAN antenna for wearable applications," *IEEE Antennas and Propagation Society International Symposium Antennas and Propagation Society International Symposium*, Vol. 2, 700–703, IEEE, Columbus, OH, USA, 2003.
20. Tronquo, A., H. Rogier, C. Hertleer, and L. V. Langenhove, "Applying textile materials for the design of antennas for wireless body area networks," *Proceedings of EuCap 2006: First European Conference on Antennas and Propagation, Nice, France*, Nov. 6–10, 2006.
21. Nageswara Rao, L. and I. Govardhani, "A cylindrical dielectric resonator antenna with meander slot for WBAN," *International Journal of Engineering and Advanced Technology*, Vol. 9, 6486–6489, 2019.
22. Raju, M. P., D. S. Phani Kishore, and B. T. P. Madhav, "CPW fed T-shaped wearable antenna for ISM band, Wi-Fi, WiMAX, WLAN and fixed satellite service applications," *Journal of Electromagnetic Engineering and Science*, Vol. 19, No. 2, 140–146, 2019.
23. Palla, R. K. and K. K. Naik, "Design of dual band antenna with defects on patch and ground for wireless applications," *International Journal of Recent Technology and Engineering*, Vol. 8, No. 2, 261–264, 2019.
24. Monik, M., S. K. Rajiya, and B. T. P. Madhav, "Fractal shaped concentric ring structured reconfigurable monopole antenna with DGS for GPS, GSM, WLAN and ISM band medical applications," *Indian Journal of Public Health Research and Development*, Vol. 9, No. 6, 285–289, 2018.
25. Raj Kamal, K. and G. Immadi, "A compact UWB micro strip patch antenna using coplanar wave guide feeding for bio medical applications," *ARPJ Journal of Engineering and Applied Sciences*, Vol. 13, No. 3, 976–981, 2018.
26. Garg, R., P. Bhartia, I. Bahl, and A. Ittipiboon, *Micrstrip Antenna Design Hand Book*, Artech House, Norwood, MA, USA, 2001.
27. Lin, I. K. C., M. H. Jamaluddin, A. Awang, R. Selvaraju, M. H. Dahri, L. C. Yen, and H. A. Rahim, "A triple band hybrid MIMO rectangular dielectric resonator antenna for LTE applications," *IEEE Access*, Vol. 7, 122900–122913, 2019.
28. Immadi, G., N. K. Majji, M. Venkata Narayana, and A. Navya, "Comparative analysis of pass band characteristics of a rectangular waveguide with and without a dielectric slab," *International Journal of Innovative Technology and Exploring Engineering*, Vol. 8, No. 6, 1209–1211, 2019.
29. Ramakrishna, T. V., B. T. P. Madhav, M. Venkateswara Rao, A. Babu Rao, A. Sunaina, A. Avinash, and B. Shivani, "SRR loaded half-mode substrate integrated waveguide monopole slot antenna for multiband applications," *International Journal of Engineering and Technology (UAE)*, Vol. 7 (1.1 Special Issue 1), 560–564, 2018.
30. Venkata Narayana, M., G. Immadi, H. Muppa, M. Nagisetty, and H. V. R. Konda, "Design of microstrip circular patch antenna array," *Journal of Advanced Research in Dynamical and Control Systems*, Vol. 9, No. 17, 2178–2185, 2017.
31. Bemani, M., S. Nikmehr, and H. Youneiraad, "A novel small triple band rectangular dielectric resonator antenna for WLAN and WiMAX applications," *Journal of Electromagnetic Waves and Applications*, Vol. 25, Nos. 11–12, 1688–1698, 2012.

32. Huang, C. L. and Y. W. Tseng, "A low-loss dielectric using CaTiO_3 -modified $\text{Mg}_{1.8}\text{Ti}_{1.1}\text{O}_4$ ceramics for applications in dielectric resonator antenna," *IEEE Transactions on Dielectrics and Electrical Insulation*, Vol. 21, 2293–2300, 2014.
33. Kha, A. A., M. H. Jamaluddin, S. Aqeel, J. Nasir, J. U. R. Kazim, and O. Owais, "A dual-band MIMO dielectric resonator antenna for WiMAX/WLAN applications," *IET Microwaves, Antennas & Propagation*, Vol. 11, 113–120, 2017.
34. Fang, X. S. and S. M. Chen, "Design of the wide dual-band rectangular souvenir dielectric resonator antenna," *IEEE Access*, Vol. 7, 161621–161629, 2019.